AIP | Applied Physics Letters

Doping suppression and mobility enhancement of graphene transistors fabricated using an adhesion promoting dry transfer process

Woo Cheol Shin, Taeshik Yoon, Jeong Hun Mun, Taek Yong Kim, Sung-Yool Choi, Taek-Soo Kim, and Byung Jin Cho

Citation: Applied Physics Letters **103**, 243504 (2013); doi: 10.1063/1.4846317
View online: http://dx.doi.org/10.1063/1.4846317
View Table of Contents: http://scitation.aip.org/content/aip/journal/apl/103/24?ver=pdfcov
Published by the AIP Publishing

Doping suppression and mobility enhancement of graphene transistors fabricated using an adhesion promoting dry transfer process

Woo Cheol Shin,[1,a)] Taeshik Yoon,[2,a)] Jeong Hun Mun,[1] Taek Yong Kim,[1] Sung-Yool Choi,[1] Taek-Soo Kim,[2,b)] and Byung Jin Cho[1,b)]
[1]*Department of Electrical Engineering, Graphene Research Center, KAIST, 373-1 Guseong-dong, Yuseong-gu, Daejeon 305-701, South Korea*
[2]*Department of Mechanical Engineering, Graphene Research Center, KAIST, 373-1 Guseong-dong, Yuseong-gu, Daejeon 305-701, South Korea*

(Received 1 October 2013; accepted 21 November 2013; published online 13 December 2013)

We present the facile dry transfer of graphene synthesized via chemical vapor deposition on copper film to a functional device substrate. High quality uniform dry transfer of graphene to oxidized silicon substrate was achieved by exploiting the beneficial features of a poly(4-vinylphenol) adhesive layer involving a strong adhesion energy to graphene and negligible influence on the electronic and structural properties of graphene. The graphene field effect transistors (FETs) fabricated using the dry transfer process exhibit excellent electrical performance in terms of high FET mobility and low intrinsic doping level, which proves the feasibility of our approach in graphene-based nanoelectronics. © *2013 AIP Publishing LLC*.
[http://dx.doi.org/10.1063/1.4846317]

Graphene has attracted extensive research interest in high speed field effect transistors (FETs) due to its exceptional mobility, high saturation velocity, and two-dimensional planar structure.[1,2] Since the discovery of graphene through the mechanical exfoliation of graphite, several methods for large area graphene synthesis including epitaxial growth on silicon carbides,[3] chemical vapor deposition (CVD)[4–7] on transition metals, and the two-dimensional assembly of reduced graphene oxides[8] have been developed. Among these methods, the CVD method has been most widely used for graphene production as it enables low-cost growth of graphene with good electrical properties. However, utilizing the CVD graphene for device applications requires a transfer step because the growth substrate is not compatible with existing device fabrication procedures. Thus far, the wet transfer method[4,5] based on the chemical etching of metals has been commonly used to deliver graphene to a functional device substrate. However, this wet process deteriorates the quality of the resulting graphene film and requires additional processes after the transfer, e.g., the removal of supporting layers and complicated graphene cleaning steps.[9]

In order to overcome these drawbacks, dry transfer methods with various adhesive layers such as thermal release tape,[10] polymers,[11] and epoxy[12] have been developed recently. The dry transfer process is highly desirable given that it exploits appropriate adhesion between the graphene and neighboring materials, and therefore enables a facile integration of the graphene into the device substrates without wet-based steps. However, the mechanism through which the interfacial adhesion property of graphene is affected has not yet been elucidated, which renders the existing dry transfer processes highly empirical. Furthermore, few graphene FETs[12] have been demonstrated using dry transfer methods and their electrical performance must be improved further in order to make the dry transfer process more feasible in graphene nanoelectronics.

In this work, the adhesion behavior of graphene to neighboring materials, including SiO_2, poly(methyl methacrylate) (PMMA), and poly(4-vinylphenol) (PVP), is systematically investigated by performing direct measurements of the adhesion energies and analyses of the molecular mechanics simulation. High quality uniform dry transfer of graphene to SiO_2 substrates was achieved through exploiting the beneficial features of a PVP adhesive layer involving a strong adhesion energy to graphene and negligible influence on the electronic and structural properties of graphene. Using the proposed dry transfer process, we further demonstrate high performance graphene FETs that exhibit superb FET mobility and charge neutrality.

For the adhesion engineering, PVP containing benzene derivatives was adopted as the adhesion promoter with the expectation of aromatic stacking on the graphene surface.[13–15] In order to quantitatively estimate the adhesive forces, we directly and precisely measured the adhesion energies of graphene to neighboring materials including the adhesion promoter, i.e., PVP. For the purpose of comparison, the measurement was also performed with SiO_2 and PMMA, which are frequently used in graphene devices as insulating substrates, supporting layers, and/or gate dielectrics.[16–23] The adhesion energy was measured using double cantilever beam (DCB) fracture mechanics testing[12] with the specimens as shown in Figure 1(a). A CVD process with inductively coupled plasma (ICP) was used for the monolayer graphene synthesis. A 300 nm-thick copper film was deposited on top of a 4-in. Si wafer covered with 300 nm-thick SiO_2, and then it was loaded into an ICP-CVD chamber. After heating in ambient Ar, the sample was exposed to H_2 plasma with a gas flow rate of 40 sccm and a RF plasma power of 50 W for 2 min. Then, a mixture of Ar and C_2H_2 (Ar:C_2H_2 = 40:1

[a)]W. C. Shin and T. Yoon contributed equally to this work.
[b)]Authors to whom correspondence should be addressed. Electronic addresses: bjcho@kaist.edu and tskim1@kaist.ac.kr.

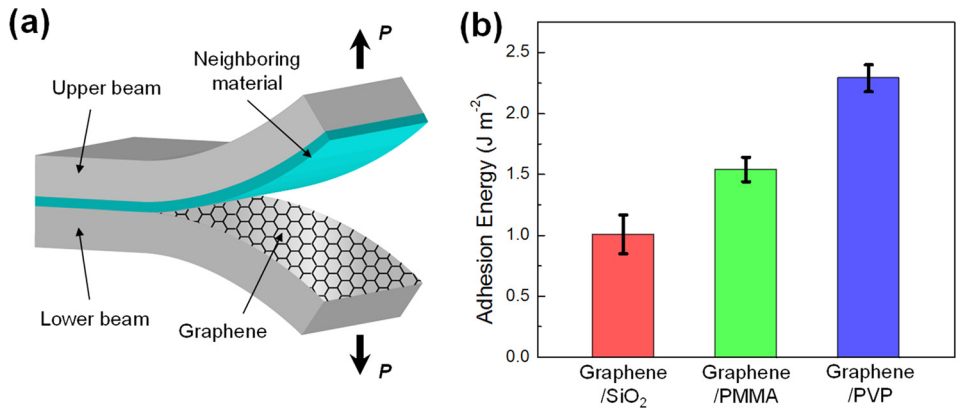

FIG. 1. (a) Schematic drawing of the DCB specimen used for measuring the interfacial adhesion energy between graphene and neighboring materials. During the test, both Si beams are loaded and unloaded at a constant displacement rate while monitoring the applied force as a function of the displacement. (b) Directly measured adhesion energy of graphene to neighboring materials (SiO_2, PVP, and PMMA). The graphene adhered to the PVP exhibits extremely strong adhesion energy of $2.31 \pm 0.11\,J/m^2$, which is more than two times higher than that of graphene on SiO_2.

sccm) was flowed into the chamber with 150 W RF plasma for the graphene synthesis process. The graphene was characterized via Raman spectra and optical transmittance, confirming that it was a high quality monolayer graphene. For the graphene-SiO_2 adhesion measurement, the graphene was transferred onto SiO_2 via the conventional layer transfer technique using chemical wet etching of Cu.[19,20] The specimen for measurement of the graphene-polymer adhesion was prepared via spin-coating polymer films on top of the as-grown graphene on the Cu.[12] The Raman spectra of the specimens before and after the DCB testing confirmed that crack growth occurred at the graphene-polymer interface during the fracture testing, which resulted in detachment of the polymer from the graphene surface.

The measured adhesion energies of graphene on SiO_2, PMMA, and PVP are shown in Figure 1(b). A graphene-SiO_2 adhesion energy of $1.02 \pm 0.17\,J\,m^{-2}$ was revealed. This value is two times larger than that of mechanically cleaved graphene on a SiO_2 substrate.[21] We attribute this discrepancy to the intrinsic defects of the CVD grown graphene,[22] which was confirmed by the presence of a D band at $1350\,cm^{-1}$ in the Raman spectra. The defect structure of the graphene involving dislocations or corrugation increased its surface energy,[23] which in turn enhanced the adhesion between the graphene and the SiO_2 substrate, although the bonding mechanism was essentially the same in that it is based on van der Waals force. The adhesion energies of $1.58 \pm 0.09\,J\,m^{-2}$ and $2.31 \pm 0.11\,J\,m^{-2}$ were measured for PMMA and PVP, respectively, which were higher than that of the graphene transferred on SiO_2. In particular, the graphene adhered to the PVP possessed an extremely strong adhesion energy that was more than two times larger than that of graphene on SiO_2. This indicates that the adhesion of graphene is controllable using the type of interfacial molecular system. In order to analyze the factors responsible for the difference in the adhesion energies, we performed a molecular mechanics simulation (ChemBio3D® Ultra) with simplified molecular models and calculated the van der Waals (vdW) energy between the graphene-polymer molecular systems. The model molecules for graphene (M_G), PMMA (M_{PMMA}), and PVP (M_{PVP}) were defined, followed by a local energy minimization. The optimized molecular configurations for each model system are shown in the inset of Figure 2, and the vdW energy is plotted as a function of the distance between the graphene and the model molecules. We found that the M_G-M_{PVP} molecular system contained aromatic rings stacked on graphene and exhibited higher vdW energy (-0.81 eV/molecule) than that of the M_G-M_{PMMA} molecular system (-0.54 eV/molecule). This tendency corresponds accurately to the experimentally measured adhesion energy ratio between the graphene-PVP and graphene-PMMA interfaces. We believe that the π-π stacking arising from the phenol (C_6H_5OH) groups in the PVP and graphene[24–26] leads to the strong vdW interaction, which is responsible for the high adhesion energy at the graphene-PVP interface. This is the experimental demonstration of the introduction of a π-stacked molecular system on a graphene surface leading to a strong vdW interaction.

The extremely strong adhesion energy at the graphene-PVP interface can be exploited for the dry transfer of

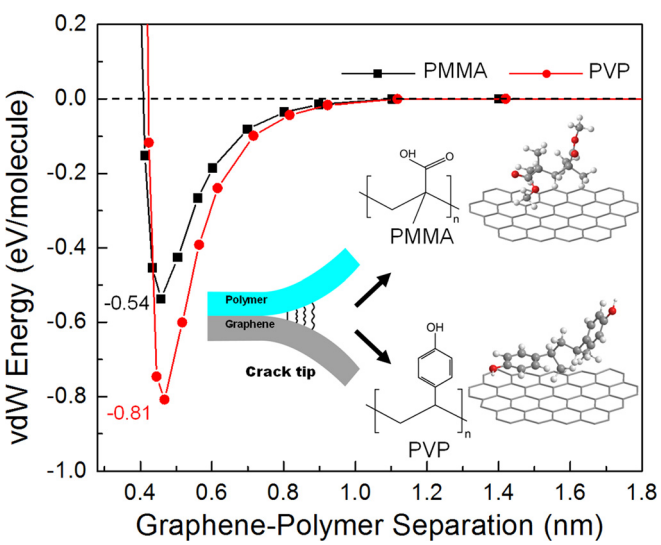

FIG. 2. The vdW energy as a function of the distance between the graphene and model molecules including M_G, M_{PVP}, and M_{PMMA}. The inset presents the chemical structures and optimized molecular configurations for each model system. The M_G-M_{PVP} molecular system with stacking of aromatic rings exhibits higher vdW energy (-0.81 eV/molecule) than that of the M_G-M_{PMMA} molecular system (-0.54 eV/molecule).

graphene. In this work, we achieved viable graphene-substrate integration where the graphene is intact and robustly integrated into the target device substrates through a facile and nondestructive dry transfer process. The process sequence in Figure 3(a) describes the dry transfer technique using the strong adhesion energy of the graphene-PVP interface. The proposed transfer process requires only a few simple steps. The PVP film was spin-coated on top of the graphene grown on a Cu substrate in order to form the adhesion promoter, which is a critical element in facilitating the subsequent delamination of the graphene. It should also be noted that the PVP film is nondestructive to both the structural and electronic characteristics of graphene, as confirmed through the Raman characterization results shown in Figure 3(b). In order to reveal the effects of the PVP coating on graphene, we performed Raman measurements before and after coating the PVP on the graphene, which was already transferred onto SiO_2 substrates using the conventional wet transfer method. We observed no change in the D-band located at $\sim 1350\,cm^{-1}$, which indicates that the PVP can be formed on graphene without introducing additional defects. Furthermore, the negligible changes in the position and full width at half maximum (FWHM) of the G-band demonstrate that the PVP induces negligible doping in the graphene.[27] The results presented in Figures 2 and 3 suggest that the π-stacked molecular system at the graphene-PVP interface can effectively enhance the interfacial adhesive strength while preserving the intrinsic properties of graphene. The PVP/graphene/Cu/Si substrate was subsequently bonded to a SiO_2 substrate using epoxy. During the subsequent mechanical delamination process, the graphene-PVP adhesion energy, which is much higher than that of the as-grown graphene on Cu ($0.72 \pm 0.07\,J\,m^{-2}$),[12] enabled the graphene to be readily separated from the Cu surface and uniformly transferred to the SiO_2 substrate. The atomic force microscopy (AFM) images demonstrate that the mechanical delamination of graphene was achieved over a large area (Figure 3(c)). The Raman spectroscopy of the graphene-delaminated Cu also confirms that the graphene was completely transferred onto the PVP film (Figure 3(d)). This suggests that the nondestructive behavior and strong adhesion energy between graphene and PVP could be exploited to provide an effective graphene integration technique for device applications.

We further demonstrate high performance graphene FETs using the abovementioned dry transfer technique with a nondestructive PVP adhesion promoter. A cross-sectional schematic view of the fabricated graphene FET is presented in Figure 4(a). The device was fabricated directly on a graphene/PVP/SiO_2 substrate prepared using the developed dry transfer technique. It is noted that the adhesion promoter, i.e., the PVP layer, should be highly cross-linked in order to resist possible damage during the subsequent device fabrication processes.[28] For comparison, we also fabricated control devices using the typical wet-based graphene transfer process. Figure 4(b) presents the transfer (I_{DS}-V_G) characteristics of the graphene FETs fabricated using the two different transfer techniques. The graphene channel layers for the dry and wet transferred devices possess strong and weak adhesion energy, respectively. The on-off current ratio of the I_{DS} of the dry transferred graphene device is two-fold higher than that of the wet transferred graphene device. For the dry transferred device, the Dirac voltage (V_{Dirac}), which depends on the doping level in the graphene,[18] is near zero while the

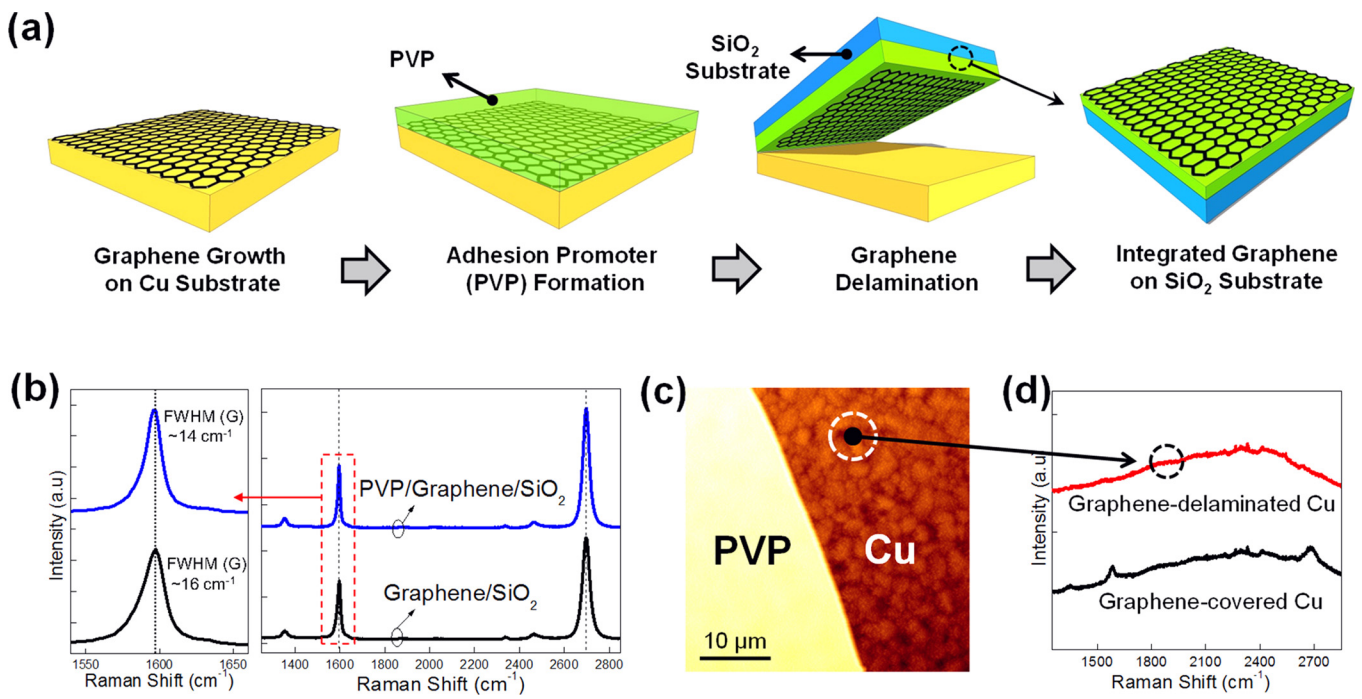

FIG. 3. (a) Process sequence of the adhesion engineered dry transfer technique. This method is composed of simple steps, yet allows the direct integration of graphene into a functional target substrate. (b) Raman spectra for graphene with and without PVP adhesion promoter. The negligible changes in the D- and G-bands demonstrate that the PVP film is nondestructive to both the structural and electronic characteristics of graphene. (c) AFM image of the boundary between the graphene-delaminated and graphene-covered Cu. (d) Raman spectroscopy for the graphene-delaminated and graphene-covered Cu demonstrating that the graphene grown on Cu is transferred completely onto the PVP/SiO_2 substrate after mechanical delamination.

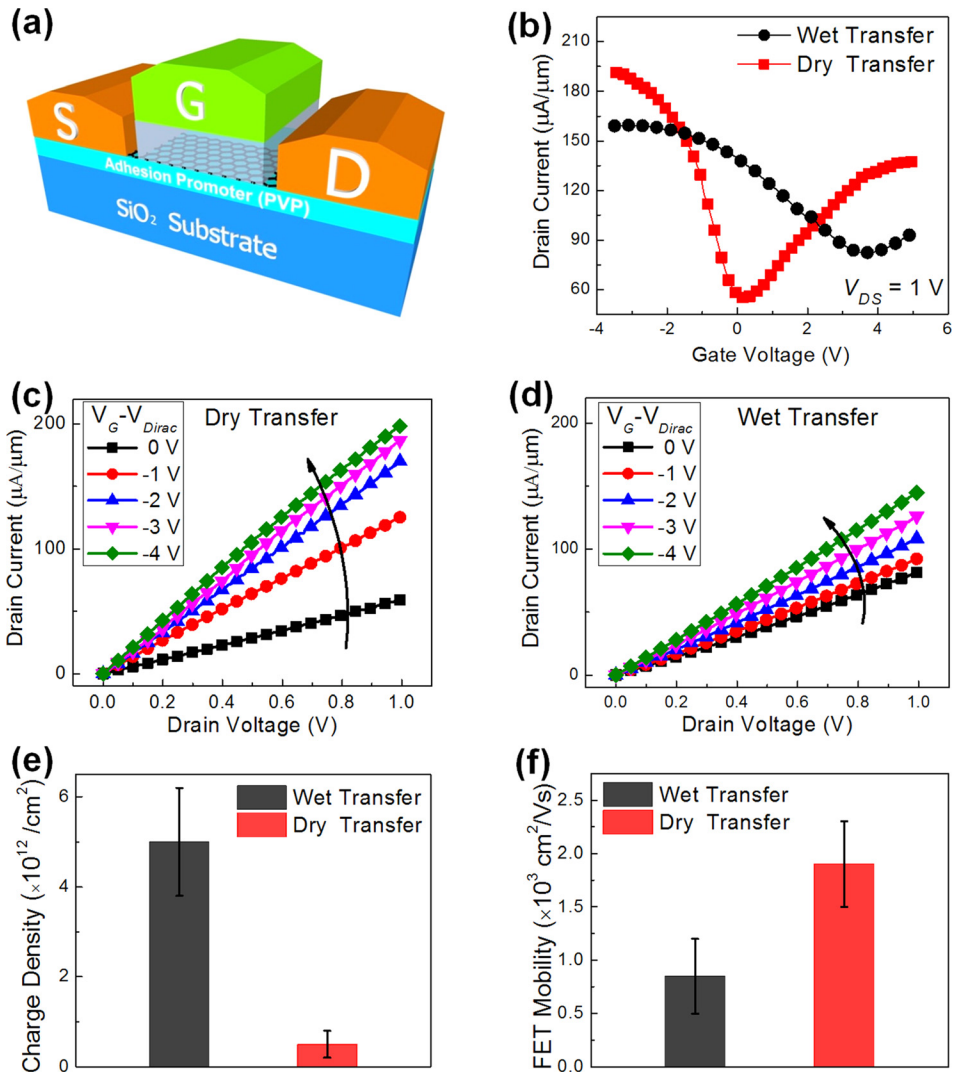

FIG. 4. Demonstration of high performance graphene FETs using the adhesion engineered graphene-substrate integration technique. (a) Schematic cross sectional view of the top-gate graphene FET on the directly integrated graphene/PVP/SiO_2 substrate. (b) Transfer characteristics (I_{DS}-V_{GS}) of the graphene FETs fabricated using two different transfer techniques. Output characteristics (I_{DS}-V_{DS}) of the (c) dry and (d) wet transferred devices. The dry transferred devices with strong adhesion energy of graphene exhibit superior electrical performance in terms of the on-off current ratio and gate modulation characteristics. The length and width of the graphene channel layer are 10 μm and 8 μm, respectively. (e) Charge density and (f) FET mobility of the graphene FETs fabricated using different transfer techniques.

V_{Dirac} of the wet transferred device shifted toward the positive direction. Figures 4(c) and 4(d) show the output characteristics (I_{DS}-V_{DS}) of the graphene FETs fabricated using the wet transfer technique and the proposed dry transfer technique. Excellent gate modulation and superior drain current drivability are consistently observed in the dry transferred devices. In order to quantitatively analyze the impact of the dry transfer technique on the FET characteristics, we extracted the charge densities and mobilities of the FETs. Figures 4(e) and 4(f) compare the charge density and FET mobility of the graphene FETs prepared using the different transfer techniques. The results demonstrate that superb charge neutrality and mobility performance were achieved using the proposed dry transfer process. We attribute the superior mobility to the intact graphene channel with good charge neutrality, which reduces the charged impurity scattering.[29,30]

In conclusion, we demonstrate that graphene adhesion can be substantially enhanced through exploiting the π-π interaction between the graphene and PVP containing benzene derivatives. The π-stacked molecular system at the graphene-PVP interface provides extremely strong adhesion energy of 2.31 ± 0.11 J m^{-2}, which is directly measured and analyzed using a molecular mechanics simulation. Using PVP as a nondestructive adhesion promoter, we developed a promising dry transfer technique through which the graphene active layer is intact and robustly integrated onto target device substrates. With our integration technique, we further demonstrate high performance graphene FETs with superb charge neutrality and FET mobility. These results will enable the intrinsic limit of graphene adhesion to be overcome and will also provide an effective approach for graphene integration, which is a prerequisite for realizing graphene-based nanoelectronic devices and systems.

This research was supported by the Basic Science Research Program through the National Research Foundation (NRF) of Korea funded by the Ministry of Education, Science and Technology (MEST: Grant Nos. 2011-0031638, 2010-0029132, and 2012R1A1A1006072).

[1]K. S. Novoselov, A. K. Geim, S. V. Morozov, D. Jiang, Y. Zhang, S. V. Dubonos, I. V. Grigorieva, and A. A. Firsov, Science **306**, 666 (2004).
[2]F. Schwierz, Nat. Nanotechnol. **5**, 487 (2010).
[3]C. Berger, Z. M. Song, X. B. Li, X. S. Wu, N. Brown, C. Naud, D. Mayo, T. B. Li, J. Hass, A. N. Marchenkov, E. H. Conrad, P. N. First, and W. A. de Heer, Science **312**, 1191 (2006).
[4]X. Li, W. Cai, J. An, S. Kim, J. Nah, D. Yang, R. Piner, A. Velamakanni, I. Jung, E. Tutuc, S. K. Banerjee, L. Colombo, and R. S. Ruoff, Science **324**, 1312 (2009).

[5]S. Bae, H. Kim, Y. Lee, X. Xu, J. Park, Y. Zheng, J. Balakrishnan, T. Lei, H. R. Kim, Y. I. Song, Y. Kim, K. S. Kim, B. Ozyilmaz, J. Ahn, B. H. Hong, and S. Iijima, Nat. Nanotechnol. **5**, 574 (2010).
[6]D. Shin, S. Bae, C. Yan, J. Kang, J. Ryu, J. Ahn, and B. H. Hong, Carbon Lett. **13**, 1 (2012).
[7]Z. Cheng, Q. Zhou, C. Wang, Q. Li, C. Wang, and Y. Fang, Nano Lett. **11**, 767 (2011).
[8]G. Eda, G. Fanchini, and M. Chhowalla, Nat. Nanotechnol. **3**, 270 (2008).
[9]X. Liang, B. A. Sperling, L. Calizo, G. Cheng, C. A. Hacker, Q. Zhang, Y. Obeng, K. Yan, H. Peng, Q. Li, X. Zhu, H. Yuan, A. R. H. Walker, Z. Liu, L. Peng, and C. A. Richter, ACS Nano **5**, 9144 (2011).
[10]J. K. Kang, S. Hwang, J. H. Kim, M. H. Kim, J. Ryu, S. J. Seo, B. H. Hong, M. K. Kim, and J. B. Choi, ACS Nano **6**, 5360 (2012).
[11]E. H. Lock, M. Baraket, M. Laskoski, S. P. Mulvaney, W. K. Lee, P. E. Sheehan, D. R. Hines, J. T. Robinson, J. Tosado, M. S. Fuhrer, S. C. Hernandez, and S. G. Walton, Nano Lett. **12**, 102 (2012).
[12]T. Yoon, W. C. Shin, T. Y. Kim, J. H. Mun, T. S. Kim, and B. J. Cho, Nano Lett. **12**, 1448 (2012).
[13]S. Wu, M. T. Gonzalez, R. Huber, S. Grunder, M. Mayor, C. Schonenberger, and M. Calame, Nat. Nanotechnol. **3**, 569 (2008).
[14]X. Dong, D. Fu, W. Fang, Y. Shi, P. Chen, and L. Li, Small **5**, 1422 (2009).
[15]A. Rochefort and J. D. Wuest, Langmuir **25**, 210 (2008).
[16]J. G. Oh, Y. Shin, W. C. Shin, O. Sul, and B. J. Cho, Appl. Phys. Lett. **99**, 193503 (2011).
[17]J. K. Park, S. M. Song, J. H. Mun, and B. J. Cho, Nano Lett. **11**, 5383 (2011).
[18]W. C. Shin, S. Seo, and B. J. Cho, Appl. Phys. Lett. **98**, 153505 (2011).
[19]W. C. Shin, T. Y. Kim, O. Sul, and B. J. Cho, Appl. Phys. Lett. **101**, 033507 (2012).
[20]S. M. Song, J. K. Park, O. Sul, and B. J. Cho, Nano Lett. **12**, 3887 (2012).
[21]S. P. Koenig, N. G. Boddeti, M. L. Dunn, and J. S. Bunch, Nat. Nanotechnol. **6**, 543 (2011).
[22]F. Banhart, J. Kotakoski, and A. V. Krasheninnikov, ACS Nano **5**, 26 (2011).
[23]Y. J. Shin, Y. Wang, H. Huang, G. Kalon, A. T. S. Wee, Z. Shen, C. S. Bhatia, and H. Yang, Langmuir **26**, 3798 (2010).
[24]S. D. Chakarova-Käck, Ø. Borck, E. Schröder, and B. I. Lundqvist, Phys. Rev. B **74**, 155402, (2006).
[25]C. A. Hunter and J. K. M. Sanders, J. Am. Chem. Soc. **112**, 5525 (1990).
[26]J. M. Hernández, E. C. Anota, M. T. de la Cruz, M. G. Melchor, and G. H. Cocoletzi, J. Mol. Model. **18**, 3857 (2012).
[27]A. Das, S. Pisana, B. Chakraborty, S. Piscanec, S. K. Saha, U. V. Waghmare, K. S. Novoselov, H. R. Krishnamurthy, A. K. Geim, A. C. Ferrari, and A. K. Sood, Nat. Nanotechnol. **3**, 210 (2008).
[28]W. C. Shin, H. Moon, S. Yoo, Y. Li, and B. J. Cho, IEEE Electron Device Lett. **31**, 1308 (2010).
[29]J. H. Chen, C. Jang, S. Adam, M. S. Fuhrer, E. D. Williams, and M. Ishigami, Nat. Phys. **4**, 377 (2008).
[30]E. H. Hwang, S. Adam, and S. D. Sarma, Phys. Rev. Lett. **98**, 186806 (2007).